Fracture Mechanics of Concrete Structures,
Proceedings FRAMCOS-2, edited by Folker H. Wittmann,
AEDIFICATIO Publishers, D-79104 Freiburg (1995)

A COMPARATIVE STUDY OF G_F TEST RESULTS

D.R. Brokenshire and B.I.G. Barr
Cardiff School of Engineering, University of Wales, Cardiff, UK

Abstract

A comparative study is reported wherein the fracture energy, G_F, has been determined, for a range of concretes, from notched beams and cylinders subjected to either torsional or flexural loading. The flexural tests were carried out on notched 500 x 100 x 100 mm beams according to the procedures given in the RILEM recommendations for the G_F test. The torsional loading arrangement used in the study provides an indirect tensile test from which G_F can be determined using the general procedure recommended by RILEM for the G_F test. In the case of the torsion tests, notches were introduced (generally to half the depth of the specimen) at an angle of 45^o to the longitudinal axis. The tests were carried out via a closed-loop system with the load controlled by the crack mouth opening displacement (CMOD) across the initial inclined notch. The load-displacement curves and/or the corresponding torque-rotation curves have been used to determine G_F for three grades of concrete corresponding to 28 day cube strengths of 40, 70 and 100 N/mm^2. The test results reported are encouraging with similar G_F values and strain softening curves being obtained from the various test geometries/loading arrangements.

1 Introduction

Three test methods for evaluating the fracture characteristics of concrete have been proposed as potential standard tests. The first is the G_F test, RILEM (1985), wherein stable bend tests are carried out on notched beam specimens subjected to three-point loading. Later, two further RILEM Draft Recommendations for fracture tests on concrete have been proposed; one is based on the Size Effect Method, RILEM (1990b), and the other on the Two Parameter Model, RILEM (1990a). All three RILEM-proposed test methods have their advantages and limitations and upon close inspection are similar in a number of their essential features. The main limitation of all three test methods is that they are more applicable for use with laboratory cast specimens than they are for use in the assessment of cores taken from existing structures.

The work reported here was initiated some three years ago and was influenced by the work of Elices and his co-workers, Guinea et al (1992), Planas et al (1992) and Elices et al (1992). They investigated systematically the potential difficulties associated with the G_F test. In particular, they considered the magnitude of the energy dissipated at the supports, inside the bulk of the most stressed regions and during the final stages of fracture. They concluded that when all these additional energies were taken into account an almost size-independent G_F value was obtained.

One of the principal objectives of the study reported here was to investigate the possibility of generalising the approach inherent in the G_F test. The G_F test is a compromise testing arrangement since the most direct method of evaluating the fracture energy, G_F, of concrete is by means of stable uniaxial tests in which the stress-deformation curve is obtained. Unfortunately, a uniaxial test is not suitable as a practical standard test. In the same way that flexural tests provide a compromise method of evaluating the fracture energy, G_F, torsional tests on notched beams and cylinders can also provide an indirect method of evaluating G_F. The torsional loading arrangement reported here (Fig. 1) provides an indirect tensile test from which G_F values can be determined using the general procedure recommended by RILEM for the G_F test. The test specimens (beams or cylinders) used in the torsion tests have notches introduced at 45^o to the longitudinal axis so that the roots of the notches are subjected to tensile stresses when the specimens are subjected to torsional loading.

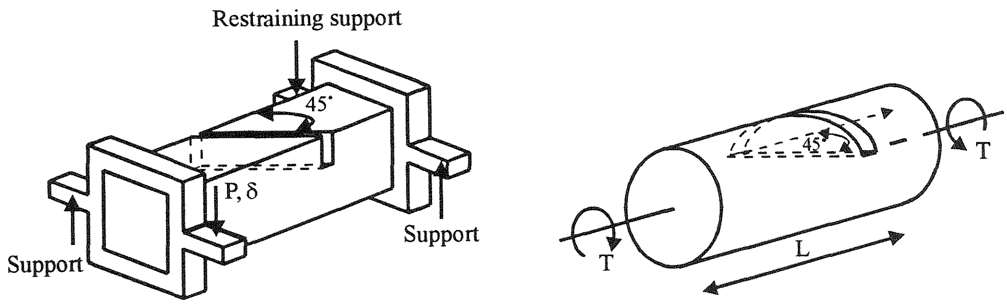

(a) Beam (b) Cylinder

Fig. 1 Schematic view of torsion tests

A second objective of the work reported here was to give due consideration to the needs of practising engineers. A brief consideration of this lead to the notion that proposed fracture tests should include a provision for such tests to be carried out on cores and cylinders. Cylindrical test specimens are normally produced with a length/diameter ratio of two or more. Cylindrical test specimens have the added advantage that they are appropriate for use where size effects are being investigated, since the compact nature of the test specimen geometry is ideally suited for such testing. Ideally, the G_F test should be carried out on compact notched cylindrical specimens subjected to three-point loading. (This approach has been pursued recently and is reported in a companion paper, Jefferson and Barr (1995).)

2 Previous work

A major objective of the experimental study was to investigate the possibility of evaluating G_F from tests carried out on notched beams or cylindrical test specimens subjected to torsional loading. The torsional loading arrangement has been reported earlier, Norris et al (1990), and is shown schematically in Fig. 1. Two supports provide upward reactions, a third support provides a downward reaction and loading is applied at the remaining free end. In the case of cylinders, the applied load is transferred into the specimens via a pair of split collars, which are bonded onto the ends of the test specimens by means of a polyester adhesive. In the case of the beam specimens, the applied load is transferred simply via collars which are hand tightened around the specimen ends.

Notches, of various depths (30, 40 or generally 50mm), were introduced into the test specimens at an angle of 45^{o} to the longitudinal axis and the test specimens were arranged so that tensile stresses were introduced at the roots of the notches upon application of the torsional load. The rotation of the test specimens was monitored directly off the specimens (but is not shown for clarity in Fig. 1), by measuring the relative displacement over a given gauge length at a fixed distance from the axis of the test specimen. Thus both load-CMOD and torque-rotation results can be obtained from the torsion tests.

In some earlier work carried out in the same laboratory, Al-Oraimi (1994) and Barr and Al-Oraimi (1993), evaluated the fracture energy of concrete (using the procedures recommended by the RILEM G_F test) from two beam geometries. One beam was the standard RILEM recommended beam (overall dimensions of 840 x 100 x 100 mm) whereas the other was a more compact standard modulus of rupture beam (overall dimensions of 500 x 100 x 100mm). The objective of the work reported by Al-Oraimi was to compare the G_F values obtained for a range of concretes via the two sizes of beams. Since the G_F values were similar, the more compact geometry could be recommended for use in National/International Codes and Standards.

3 G_F tests

As stated earlier, the G_F test has a number of advantages and limitations. Its main advantages are its simplicity and its potential for practical application. The test is carried out on a notched beam, in three-point loading, and a readily understood fracture parameter (G_F) is obtained. Furthermore, the test can readily be extended to include the determination of the elastic modulus and the tensile strength as well as the strain softening response of the concrete.

Another obvious advantage of the G_F test is that it provides directly the softening curve for a particular concrete. The shape of the descending branch of the load-deflection curves gives an indication of the toughness of the concrete. Various brittleness numbers (based on ratios of various parameters given by load-deflection curves) have been proposed as indicators of brittleness and more recently Tran Tu and Kasperkiewicz (1994) have introduced the notion of a Shape Index (S_T) to characterise the softening curves for various grades of concrete.

In numerical modelling, the softening function is the main input requirement to model the fracture of concrete when using the cohesive crack model approach. As reported recently by Guinea et al (1994), the simplest method of obtaining the softening curve is via direct tensile tests but such tests have many limitations since it is difficult to achieve stable crack propagation. Hence most methods used to determine softening curves are indirect methods, Wittmann (1988). Yet more examples of the use of indirect methods to determine softening curves are reported here.

The G_F test also has a number of disadvantages. One of its disadvantages is that G_F values are very similar for low, medium and high strength concrete. The G_F values do not distinguish between various grades of concrete whereas the shape of the softening curve does reflect the difference in brittleness. Another potential difficult with the G_F test is the recommendation of a large span-to-depth ratio in order to ensure stable crack propagation. However, the use of a good closed-loop testing machine overcomes this practical difficulty and much more compact test geometries can be used. Last, but not least, the G_F test (as well as the SEM and the TPM) has been developed in well equipped laboratories and all test specimens are readily prepared in beam moulds in the concrete laboratory. This situation is somewhat different to that facing the practising engineer who has the task of assessing the current fracture properties of the concrete and the probable remaining life of the structure. In such cases it is normal practice to take cores from the structures in order to evaluate the state of the concrete. These practical considerations influenced the decisions regarding the type of test specimen geometries used in this study.

4 Experimental details

Flexural tests were carried out on notched 500 x 100 x 100 mm beams according to the general procedures described in the RILEM recommendations for the G_F test. Two other test geometries (notched beams 500 x 100 x 100 mm and cylinders up to 500 mm long and 100 mm diameter) subjected to torsional loading resulting in an indirect tensile test being performed on the test specimen were also used in the study (see

Fig. 1). All tests were carried out in a closed-loop machine, in a stable manner, and a number of softening curves were produced from each test.

In the case of the cylinders subjected to torsion, notches of various depths were introduced at an angle of 45^{o} to the longitudinal axis and the test specimens were arranged so that the root of the notches was subjected to tension due to the torsional loading arrangement. The rotation due to the applied torque was measured directly off the cylinders by recording the relative displacement (via an LVDT) over a given gauge length at a fixed distance away from the axis of the cylinder. The gauge length was determined by the distance between a pair of steel rings (located concentrically with the test specimen via three locating screws) positioned adjacent, but within, the loading collars.

The general testing arrangements for the notched beam specimens subject to torsion were the same as for the cylinders. One advantage of the beam specimens is that there is no need to use glue to attach the split collars used to apply the load. As in the case of cylinders, notches of various depths were introduced into the beams and the rotation was again determined directly off the test specimens.

The same four mixes (Table 1) were used for all three test geometries. Three grades of concrete (nominal 40, 70 and 100 N/mm^2 at 28 days) were used in the study. The fine aggregate was a local sea-dredged sand and the coarse aggregate was crushed limestone (10mm) for three of the mixes and gravel (also 10mm) for the fourth mix. In the case of the nominal 100 N/mm^2 concrete, microsilica in slurry form (50 : 50 slurry) was used together with a superplasticizer (Complast 430).

Table 1 Mix details (Proportion by weight)

Concrete Grades	Cement	Fine	Coarse	Water	Microsilica
40	1	2	2.5	0.55	-
70	1	2	2.5	0.35	-
70 (Gravel)	1	2	2.5	0.35	-
100	1	1.34	2.24	0.30	10

In the case of the beams in flexure, three softening curves were obtained during the tests, as follows:

P - δ curve i.e. normal load-deflection curve for G_F test.

P - CMOD curve i.e. load-crack mouth opening displacement.

P - δ_{RAM} curve i.e. load-ram deflection.

In the case of the beams and cylinders in torsion, three softening curves were also produced during the tests, as follows:

$P - \delta$ curve i.e. equivalent to torque-rotation curve.

P - CMOD curve i.e. load-crack mouth opening displacement.

$P - \delta_{RAM}$ curve i.e. load-ram deflection.

In some of the torsion tests, the displacement normal to the crack-mouth opening displacement was also determined so that any possible Mode II type of displacement could be investigated. Thus a number of softening curves were produced from each test and the relative energy associated with each is considered in the next section.

5 Results and discussion

Typical softening curves for the three grades of concrete used in the study are shown schematically in Fig. 2. The left hand figures show the $P - \delta$ relationships from which the G_F values can be determined according to the RILEM recommendations. (In the case of the beams and cylinders in torsion the equivalent torque-rotation ($T - \phi$) relationships have been used to determine G_F.) The middle column of figures shows the P - CMOD relationships and the shape of these softening curves is identical to those given by the $P - \delta$ (or $T - \phi$) curves. Fig. 2 also shows (right hand figures) the $P - \delta_{RAM}$ relationships from which the apparent total work done during the tests can be determined. Since the main theme of the work reported here is to provide a comparative study for G_F values, the results presented in Tables 2-4 are in terms of the work done (given by the areas under the curves shown in Fig. 2) rather than in terms of the actual G_F values.

The problems associated with the accurate determination of energy consumed at the end of the softening curve have been known for some time. Elices et al (1992) have shown that this energy cannot be neglected for small specimens and that where it is taken into account the actual $G_F$values appear to be virtually size-independent. Some thought had to be given to the influence of the tail of the softening curves obtained in the torsion tests and, in particular, at what stage the $P - \delta$ tail could be cut. Fig. 3 shows a plan view of the torsion test loading arrangement. If $L > x$ (which was the case in all the tests reported here) then the self weight of the test specimens provides a closing moment across the crack face. It has

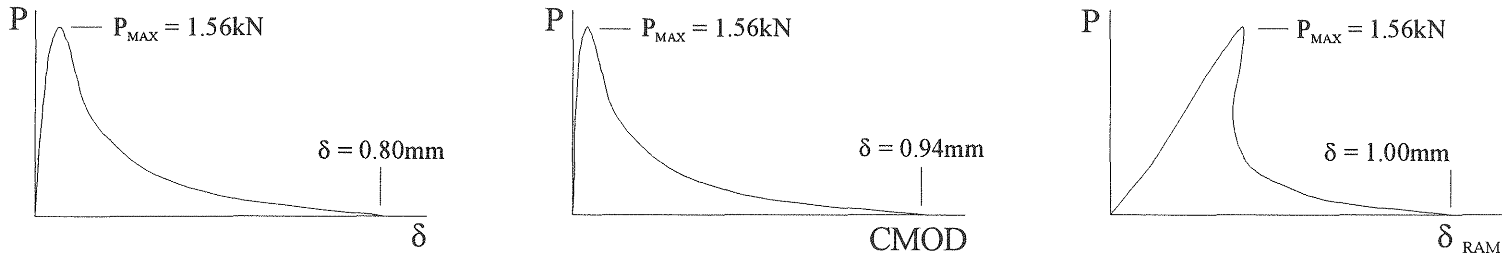

(a) Beams in bending (Grade 40 concrete)

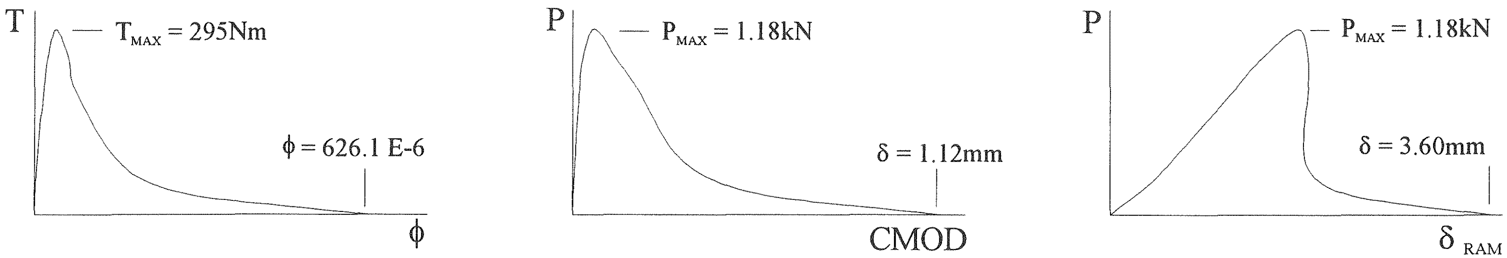

(b) Cylinders in torsion (Grade 70 concrete)

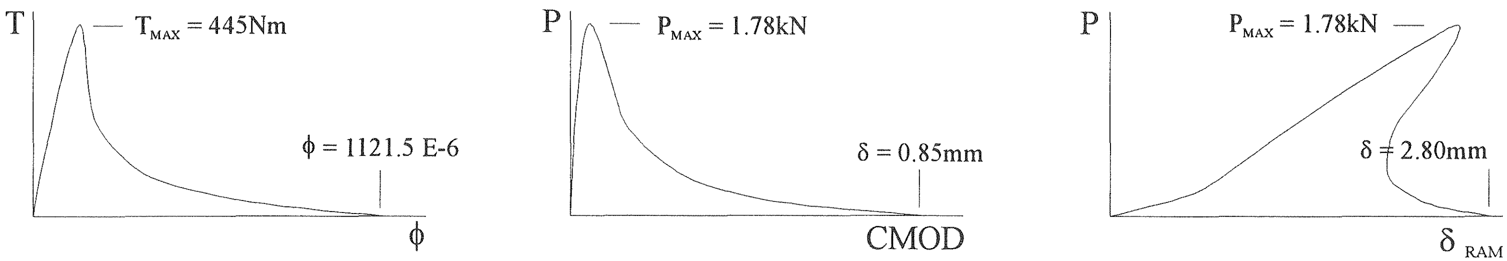

(c) Beams in torsion (Grade 100 concrete)

Fig.2. Typical softening curves for the three grades of concrete (50mm notch and limestone agg.)

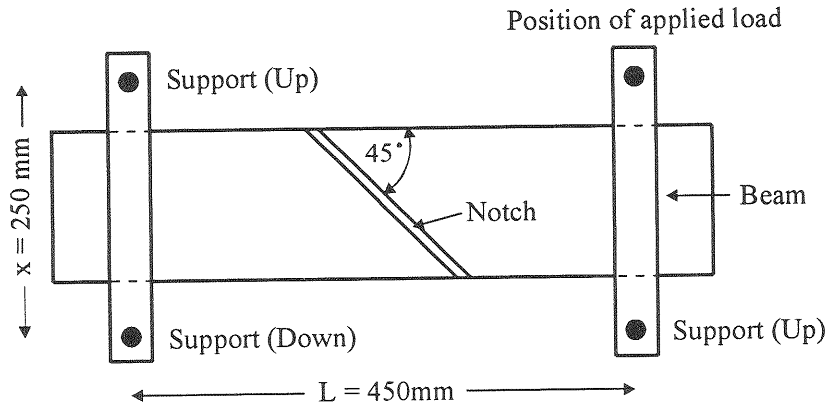

Fig. 3 Plan view of torsional testing arrangement

been assumed here that where the P - δ tail become horizontal, the closing moment due to self weight was balanced by the applied torque and the test could be considered to be completed. Furthermore, since this was a comparative study of G_F (based on Work Done) continuing the tests beyond this point was not necessary.

The results for the Work Done, given by the three softening curves, for the four types of concrete are summarised in Tables 2, 3 and 4. Column

Table 2 Summary of Work Done for Beams in Bending

Concrete Grade (N/mm^2)	Notch Depth (mm)	G_F (N/m)	Work Done (Nm) P-δ (V%)	P-CMOD (V%)	$\frac{P\text{-}\delta}{P\text{-CMOD}}$ (V%)	$P\text{-}\delta_{RAM}$ (V%)	$\frac{P\text{-}\delta}{P\text{-}\delta_{RAM}}$ (V%)
40	50	83.9 (9.1)	0.307 (10.7)	0.300 (10.8)	1.026 (7.2)	0.449 (15.8)	0.693 (15.2)
	30	107.1 (12.0)	0.600 (13.0)	0.542 (11.6)	1.107 (6.2)	0.826 (22.0)	0.748 (18.4)
70	50	108.4 (7.0)	0.419 (6.1)	0.379 (7.1)	1.106 (2.3)	0.551 (25.0)	0.795 (22.7)
	30	104.4 (9.0)	0.613 (7.9)	0.526 (6.9)	1.166 (4.5)	0.838 (17.5)	0.753 (21.9)
70 GRAVEL	50	121.7 (23.5)	0.456 (24.6)	0.412 (19.6)	1.098 (5.7)	0.637 (23.1)	0.781 (12.6)
	30	126.4 (7.9)	0.714 (8.4)	0.615 (4.5)	1.160 (6.2)	0.840 (25.9)	0.888 (12.1)
100	50	104.2 (9.0)	0.404 (8.2)	0.329 (7.3)	1.229 (3.1)	0.558 (14.8)	0.732 (10.5)
	40	96.9 (16.0)	0.469 (15.7)	0.406 (13.4)	1.156 (7.4)	0.599 (31.3)	0.809 (14.3)

Table 3 Summary of Work Done for Cylinders in Torsion

Concrete Grade (N/mm^2)	Notch Depth (mm)	G_F * (N/m)	Work Done (Nm)				
			P-δ (V%)	P-CMOD (V%)	P-δ P-CMOD (V%)	P-δ_{RAM} (V%)	P- δ P-δ_{RAM} (V%)
40	50	46.3	0.046	0.257	1.178	0.811	0.059
			(32.8)	(11.3)	(28.5)	(12.8)	(31.7)
	30	60.5	0.116	0.508	0.226	1.959	0.059
			(15.6)	(12.2)	(13.0)	(16.8)	(20.2)
70	50	55.8	0.072	0.310	0.226	1.467	0.055
			(53.3)	(16.7)	(42.2)	(32.2)	(69.1)
	30	59.0	0.212	0.496	0.441	2.417	0.090
			(16.0)	(10.2)	(25.5)	(7.6)	(17.5)
70 GRAVEL	50	73.6	0.083	0.409	0.194	1.138	0.067
			(41.9)	(11.0)	(44.0)	(16.7)	(40.0)
	30	84.9	0.283	0.713	0.424	2.463	0.125
			(16.3)	(18.1)	(37.8)	(13.8)	(35.2)
100	50	46.6	0.051	0.259	0.199	2.003	0.026
			(21.4)	(6.6)	(15.3)	(7.9)	(17.1)
	40	49.2	0.097	0.346	0.283	3.057	0.031
			(60.9)	(7.2)	(63.4)	(14.6)	(46.6)

*Provisional results

Table 4 Summary of Work Done for Beams in Torsion

Concrete Grade (N/mm^2)	Notch Depth (mm)	G_F * (N/m)	Work Done (Nm)				
			P-δ (V%)	P-CMOD (V%)	P-δ P-CMOD (V%)	P-δ_{RAM} (V%)	P- δ P-δ_{RAM} (V%)
40	50	83.8	0.395	0.424	0.927	1.243	0.318
		(18.9)	(20.5)	(15.0)	(10.2)	(18.8)	(11.1)
	30	82.8	0.495	0.571	0.876	1.930	0.262
		(14.6)	(17.3)	(20.3)	(9.9)	(22.8)	(16.9)
70	50	90.1	0.419	0.458	0.912	1.462	0.287
		(19.5)	(20.4)	(15.9)	(12.5)	(18.6)	(12.6)
	30	103.4	0.682	0.717	0.960	4.166	0.167
		(9.0)	(12.5)	(8.1)	(17.4)	(16.1)	(20.0)
70 GRAVEL	50	114.1	0.498	0.589	0.820	1.736	0.278
		(36.0)	(42.2)	(21.9)	(24.3)	(17.1)	(27.7)
	30	110.6	0.655	0.868	0.747	3.205	0.204
		(29.1)	(36.4)	(10.4)	(29.7)	(16.2)	(29.9)
100	50	58.1	0.254	0.315	0.803	1.676	0.158
		(11.5)	(13.9)	(6.3)	(9.3)	(29.5)	(22.4)
	40	67.1	0.351	0.421	0.835	2.936	0.122
		(9.7)	(11.3)	(8.0)	(10.9)	(18.5)	(14.0)

*Provisional results

five in each Table gives the ratio between the P - δ curves and the P - CMOD curves. In the case of the beams in bending (Table 2) the ratio between P - δ and P - CMOD is approximately of the order of 1.1. If we assume that the final shape of the cracked beams can be considered as two rigid half-beams pivoting around a hinge of the point of application of the load, as illustrated in Fig. 4, a simple relationship between δ and CMOD can be assumed to be given by CMOD = $(4D/S)\delta$. In the case of the beams tested here, D = 100mm and S = 450 mm and hence CMOD = 0.89 δ. In other words, if all the results for the Work Done given by the P - CMOD curves are scaled up by a factor of 1.125 the actual G_F.values will be obtained. Thus the results presented in Table 2 suggest that the P - CMOD graphs can be used as an indirect method of evaluating G_F.values. We also note that the shape of the softening curves are identical for the P - δ and P - CMOD graphs.

A similar analysis of the ratio between P - δ and P - CMOD results from the torsion tests is under way at the time of writing. The relationship is not so clear in this case and the ratio appears to be dependent on the initial notch depth. Furthermore, the relationships appear to be more uniform and predictable in the case of the beam in torsion (Table 4) than in the case of the cylinders in torsion (Table 3).

In Table 4 the Work Done, from the P - δ curve, has been converted into the equivalent Work Done as defined by the torque-rotation. This Work Done was divided by the actual (rather than nominal) crack area to give G_F. Although there was evidence of Mode II displacement during cracking, this effect has been ignored in evaluating G_F. The G_F results in Tables 2 and 4 are (with one exception) in good agreement. Similarly, the

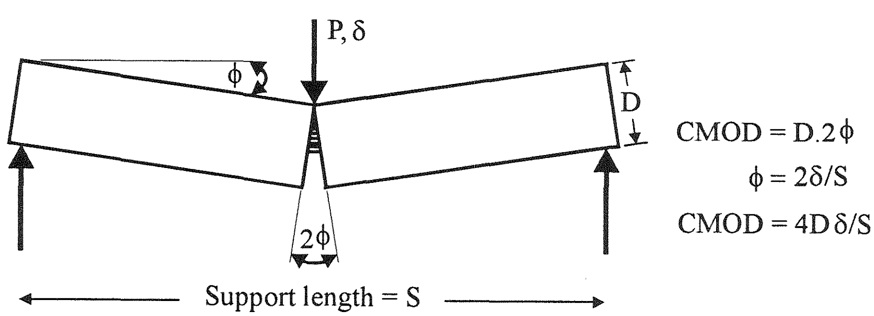

Fig. 4 Schematic view of beam at end of G_F test

Work Done given by P - CMOD curves in Tables 2 and 4 are in good agreement, when allowance is made for the difference in cracked areas.

Unfortunately, only the P - CMOD curves for the cylinders (Table 3) show good agreement with results from other specimens. In Table 3 the Work Done based on the P - CMOD curves has been used to estimate the G_F results. Further work is required in this area before drawing firm conclusions.

The additional work consumed in a fracture test, over and above that absorbed during crack propagation, has been investigated by numerous researchers. For example, Planas et al (1992) have evaluated the energy dissipation at the point of application of the applied central load in the G_F test and have concluded that this is less than 10% of the G_F energy even for the largest test specimens. In this study an attempt has been made to measure the actual energy dissipation as recorded by the deflection of the ram position of all three test geometries. This energy is shown in the form of Work Done in Tables 2 - 4 and its ratio to the Work Done as determined from the P - δ curves is given in the last column of the tables. The results for the beams in bending (Table 2) show that the Work Done as measured by the P - δ_{RAM} curves is up to 50% greater than that determined from the P - δ curves. These results confirm the importance of measuring displacements directly off the test specimens in fracture tests. These results together with some earlier work, Elices et al (1992), also suggest that the P - CMOD curves could be a better indirect method of evaluating G_F than the current proposed method. The corresponding results for the ratio P - δ/P - δ_{RAM} given in Tables 3 and 4 are much more variable and their analysis is under way at the time of writing.

6 Conclusions

The initial results whereby both P - δ and P - CMOD curves have been produced in the traditional type of G_F testing arrangement for beams in flexure are most encouraging. The test results suggest that the P - CMOD curve is sufficient to evaluate G_F and can also be used to indicate the exact form of the softening curve for use in numerical modelling. If this result is repeated for all test specimen sizes, then the need for a yoke arrangement in order to determine the actual beam deflection is eliminated. Furthermore, the integration of the G_F test with that of the Two Parameter Model test method will follow naturally if the identical nature of the P - δ and P - CMOD curves is confirmed.

The experimental results for the cylinders and beams in torsion have been somewhat disappointing. Although the P - δ curves and the P - CMOD curves are similar in nature (and also similar to those obtained in the G_F tests) the G_F values, unfortunately, show large variations. Further detailed work is required to provide direct relationships between the P - CMOD curves and the torque-rotation curves and hence the G_F values.

The results presented here for the P - δ_{RAM} curves show the significant over-estimate of Work Done to cause fracture on the basis of the apparent external work done calculated using the load and ram displacement. These results provide quantitative data for what has been known qualitatively for some time. The overestimate of Work Done given by the P - δ_{RAM} curves is of the order of 30 - 50%.

The analysis of the significant experimental data reported here is continuing. In particular, the possible use of the torque - CMOD curves for evaluating the actual G_F values is continuing. The possible effects of crack mouth sliding, due to a Mode II displacement component, is also being pursued. Once these difficulties have been resolved the torque - CMOD curves could provide G_F values as well as a description of the softening curves.

7 References

Al-Oraimi, S.K.A. (1993) **Study of concrete brittleness**, PhD Thesis, University of Wales, pp 372.

Barr, B. and Al-Oraimi, S.K.A. (1994) Fracture energy of concrete, in Proceedings International Symposium, **Brittle Matrix Composites 4** (Eds. A.M. Brandt, V.C. Li and I.H. Marshall) IKE and Woodhead Publishers, Warsaw, pp 81-90.

Elices, M., Guinea, G. and Planas, J. (1992) Measurement of the fracture energy using three point bend tests : 3. Influence of cutting of the P - δ tail, **Materials and Structures**, 25, pp 327-334.

Guinea, G., Planas, J. and Elices, M. (1992) Measurement of the fracture energy using three point bend tests : 1. Influence of experimental procedures, **Materials and Structures**, 25, pp 212-218.

Guinea, G.V., Planas, J. and Elices, M. (1994) A general bilinear fit for the softening curve of concrete, **Materials and Structures**, 27, pp 99-105.

Jefferson, A.D. and Barr, B. (1995) Unified test procedure for evaluating the fracture characteristics of concrete, **Proceedings FRAMCOS 2**, AEDIFICATIO Publishers, Switzerland.

Norris, P., Wood, J.G.M. and Barr, B. (1990) A torsion test to evaluate the deterioration of concrete due to alkali-aggregate reaction. **Magazine of Concrete Research**, 42, (153), 239-244.

Planas, J., Elices, M. and Guinea, G. (1992) Measurement of the fracture energy using three point bend tests : 2. Influence of bulk energy dissipation, **Materials and Structures**, 25, pp 305-312.

RILEM Draft Recommendation (1985) Determination of the fracture energy of mortar and concrete by means of three point bend test on notched beams, **Materials and Structures**, 18, pp 285-290.

RILEM Draft Recommendation (1990a) Determination of the fracture parameters (K_{Ic} and $CTOD_c$) of plain concrete using three point bend tests, **Materials and Structures**, 23, pp 457-460.

RILEM Draft Recommendation (1990b) Size effect method for determining fracture energy and process zone size of concrete, **Materials and Structures**, 23, pp 461-465.

Tran Tu, V. and Kasperkiewicz (1994) The relationship between stress and crack opening in fracture of concrete, in Proceedings International Symposium, **Brittle Matrix Composites 4** (Eds. A.M. Brandt, V.C. Li and I.H. Marshall) IKE and Woodhead Publishers, Warsaw, pp 219-228.

Wittmann, F.H., Rokugo, K., Bruhwiler, E., Mihashi, H. and Simoni, P. (1988) Fracture energy and strain softening of concrete as determined by means of compact tension specimens **Materials and Structures**, 21, pp 21-32.